A Journal of the Gesellschaft Deutscher Chemiker

Angewandte International Edition GDCh Chemie

www.angewandte.org

Accepted Article

Title: Dinuclear Metal Synergistic Catalysis Boosts Photochemical CO2-to-CO Conversion'

Authors: Ting Ouyang, Hong-Juan Wang, Hai-Hua Huang, Jia-Wei Wang, Song Guo, Wen-Ju Liu, Di-Chang Zhong, and Tong-Bu Lu

To be cited as: *Angew. Chem. Int. Ed.* 10.1002/anie.201811010
Angew. Chem. 10.1002/ange.201811010

Link to VoR: http://dx.doi.org/10.1002/anie.201811010
http://dx.doi.org/10.1002/ange.201811010

WILEY-VCH

10.1002/anie.201811010

Angewandte Communications

CO_2 Reduction

Dinuclear Metal Synergistic Catalysis Boosts Photochemical CO_2-to-CO Conversion

Ting Ouyang,[1,3,†] Hong-Juan Wang,[1,†] Hai-Hua Huang,[2] Jia-Wei Wang,[2] Song Guo,[1] Wen-Ju Liu,[2] Di-Chang Zhong,*[,1] and Tong-Bu Lu*[,1,2]

***Abstract**: The solar-driven CO_2 reduction is a perennial challenge in the field of 'artificial photosynthesis', as most of the reported catalysts display low activity and selectivity for CO_2 reduction in water-containing reaction systems due to competitive proton reduction. Herein, we report a dinuclear heterometallic complex, $[CoZn(OH)L^1](ClO_4)_3$ (**CoZn**), which shows extremely high photocatalytic activity and selectivity for CO_2 reduction in water/acetonitrile solution. It achieves a selectivity of 98% for CO_2-to-CO conversion, with TON and TOF values of 65000 and 1.8 s^{-1}, respectively, 4, 19 and 45-fold higher than the values of corresponding dinuclear homometallic $[CoCo(OH)L^1](ClO_4)_3$ (**CoCo**), $[ZnZn(OH)L^1](ClO_4)_3$ (**ZnZn**) and mononuclear $[CoL^2(CH_3CN)](ClO_4)_2$ (**Co**) respectively under the same conditions. The increased photocatalytic performance of **CoZn** is due to the enhanced dinuclear metal synergistic catalysis (DMSC) effect between Zn^{II} and Co^{II}, which dramatically lowers the activation barriers of both transition states of CO_2 reduction.*

Dinuclear metal catalyst, where two closely associated metal sites within one catalyst, usually shows higher catalytic activity than the mononuclear counterpart due to the dinuclear metal synergistic catalysis (DMSC) effect between two metal sites.[1-5] Compared with mononuclear metal catalyst, the dinuclear one bears more parameters to optimize its catalytic performances, not only by changing the metal and ligand, but also varying the bimetallic pairing.[5] In biological systems, many catalytic active centers of metalloenzymes are dinuclear metallic complexes,[6-7] such as heterometallic $[NiFe_4(OH)S_4]$ cluster-based carbon monoxide dehydrogenase (CODHs), dinuclear-Fe(II)-based hydrogenase, dinuclear-Cu(II)-based tyrosinase and laccase, dinuclear-Zn(II)-based alkaline phosphatase, dinuclear-Cu-Zn bovine superoxide dismutase, and so on. By exploiting metal-metal cooperativity to accomplish different substrate recognition and transformation, these metalloenzymes undertake diverse physiologic functions in life system. In previous investigations, we and others have found that some dinuclear metal complexes with close M···M distance display synergistic effect for the recognitions and activation/catalysis of small molecules and anions.[8-14] In addition, it has been found that the addition of Lewis acidic metal cations to the mononuclear metal electrocatalysts can lower the overpotentials and subsequently increase the activities for the electrocatalytic CO_2 reduction.[15-17]

The solar-driven reduction of CO_2 into chemical fuels/feedstocks represents a potential strategy for solving the issues of energy crisis and global warming caused by increasing CO_2 emission.[18-25] The critical bottleneck of this project is to develop cheap catalysts that can selectively and effectively reduce CO_2 into a single chemical fuel/feedstock.[26-27] Although a large number of mononuclear molecular photocatalysts for CO_2-to-CO conversion have been developed during the past several decades, most of the catalysts display relatively low efficiency and selectivity (Table S1). Particularly in water-containing catalytic systems, the efficiency and selectivity are even lower due to the competitive reaction of proton reduction (Table S1).[28-32] Recently, we reported a dinuclear molecular catalyst of $[CoCo(OH)L^1](ClO_4)_3$ (**CoCo**),[18] which displays much higher photocatalytic activity (TON = 16896) and selectivity (98%) than the corresponding mononuclear complex of $[CoL^2(CH_3CN)](ClO_4)_2$ (**Co**, TON = 1600 with 85% selectivity) for the reduction of CO_2 to CO in H_2O/CH_3CN (L^1 = $N[(CH_2)_2NHCH_2(m\text{-}C_6H_4)CH_2NH(CH_2)_2]_3N$, L^2 = *N*,*N*',*N*"-tris(2-benzylaminoethyl)amine, Figure 1), probably due to the DMSC effect between two Co^{II} ions, that is, one Co^{II} serves as a catalytic center, and the other Co^{II} acts as an assistant catalytic site to facilitate the cleavage of C-O bond of the O=C-OH intermediate. As the coordination environments of both Co^{II} in **CoCo** are identical, it is unable to identify the catalytic center and the assistant catalytic site in **CoCo**, thus the proposed DMSC effect within dinuclear **CoCo** need to be further investigated and confirmed.

To give direct evidence for this significant DMSC, herein, we designed and synthesized a dinuclear heterometallic cryptate, $[CoZn(OH)L^1](ClO_4)_3$ (**CoZn**), in which one Co^{II} in **CoCo** was replaced by a Zn^{II}. The selection of Zn^{II} is based on the following considerations: (1) The Zn^{II} has little catalytic activity for photochemical reduction of CO_2 to CO. The possible enhanced photocatalytic activity of **CoZn** catalyst over **Co** would give direct evidence for the existence of DMSC effect within dinuclear metal cryptates. (2) The Zn^{II} possesses stronger binding affinity to OH^- than Co^{II}, which implies that the cleavage of C-OH bond in O=C-OH intermediate by **CoZn** would be easier, and the DMSC effect within **CoZn** would be strengthened (Figure S1). As expected, though Zn^{II} itself has little photocatalytic activity, the stronger binding affinity of Zn^{II} to OH^- greatly strengthens the DMSC effect between Co^{II} and Zn^{II}, thus significantly enhances the activity of **CoZn** for photocatalytic reduction of CO_2 to CO. The TON and TOF values reach 65000 and 1.80 s^{-1}, respectively, 4, 19 and 45-

[*] Dr. T. Ouyang[+], Dr. H. J. Wang[+], S. Guo, Prof. D. C. Zhong, Prof. T. B. Lu
Institute for New Energy Materials and Low Carbon Technologies, School of Materials Science and Engineering, Tianjin University of Technology, Tianjin 300384, China.
E-mail: zhong_dichang@hotmail.com; lutongbu@tjut.edu.cn
Dr. H. H. Huang, J. W. Wang, W. J. Liu, Prof. T. B. Lu
MOE Key Laboratory of Bioinorganic and Synthetic Chemistry, School of Chemistry, Sun Yat-Sen University, Guangzhou 510275, China
Dr. T. Ouyang
School of Chemistry and Chemical Engineering, Guangzhou University, Guangzhou 510006, China.
† These authors contributed equally to this work.

Supporting information (SI) for this article is available on the WWW under http://dx.doi.org/10.1002/anie.201xxxxxx.

Angewandte Communications

fold higher than the corresponding TON and TOF values achieved by **CoCo**, **ZnZn** ([ZnZn(OH)L^1](ClO$_4$)$_3$) and **Co**, respectively. Further investigation revealed that simply adding Zn^{II} as a Lewis acid to the reaction system containing mononuclear **Co** or dinuclear **CoCo** catalyst cannot boost the photocatalytic activity for CO_2-to-CO conversion. The strengthened DMSC effect and subsequently enhanced catalytic activity of **CoZn** for photochemical reduction of CO_2 to CO were supported by DFT calculations.

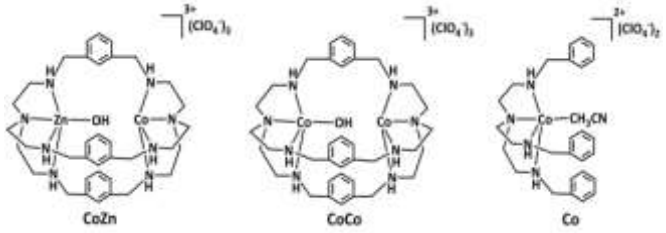

Figure 1. Structures of designed molecular catalysts, (a) dinuclear **CoZn**; (b) dinuclear **CoCo**; (c) mononuclear **Co**.

The **CoZn** cryptate was synthesized by the reaction of L^1 with Zn^{II} and Co^{II} step by step (see the supporting information, SI). Electrospray ionization mass spectrometry (ESI-MS) clearly shows that the mononuclear Zn^{II} complex of [ZnL^1]$^{2+}$ was generated at the first step (Figure S2a). After further reaction of [ZnL^1]$^{2+}$ with Co^{II}, a carbonate-bridged complex of [CoZn(μ-CO$_3$)L^1](ClO$_4$)$_2$ (**CoZn-a**) was formed, which was demonstrated by the result of ESI-MS measurement. As shown in Figure S2c, the ion peak at m/z = 390.65 corresponds to the species of [CoZn(CO$_3$)L^1]$^{2+}$. The absence of the ion peaks corresponding to [CoCo(CO$_3$)L^1]$^{2+}$ and [ZnZn(CO$_3$)L^1]$^{2+}$ rules out the possibility for the formation of a mixture of [CoCo(CO$_3$)L^1]$^{2+}$ and [ZnZn(CO$_3$)L^1]$^{2+}$, demonstrating that the dinuclear heterometallic **CoZn-a** has been successfully obtained. Similar to **CoCo**,[18] the suitable Co···Zn distance of 5.56 Å in **CoZn** cryptate (Figure S3), obtained from the optimized structure of **CoZn-a** (see the results of DFT calculations), is favorable for the formation of a μ-CO$_3^{2-}$ bridged cryptate of **CoZn-a** within its cavity. However, compared to **CoCo**, **CoZn** is much easier to absorb atmospheric CO_2 at room temperature to form μ-CO$_3^{2-}$ bridged cryptate, thus **CoZn** can only be obtained in a glove box under nitrogen atmosphere with CO_2-free solvents. Trace amount of atmospheric CO_2 will lead to the formation of **CoZn-a** (Figure S2e). The rapid absorption and fixation of atmospheric CO_2 suggests that **CoZn** bears stronger affinity towards CO_2 substrate than **CoCo**. The results of XPS and ICP-AES measurements reveal that the valence of Co and Zn is +2 (Figure S4), and the Co/Zn molar ratio in the synthesized **CoZn-a** is 1:1 (Table S2). As **CoZn-a** is the only component originated from **CoZn** by rapid absorption of atmospheric CO_2, and is stable under the general experimental conditions, thus we used substrate-bonded **CoZn-a** instead of **CoZn** as the starting material for the subsequent investigations. UV-vis spectra and the cyclic voltamemetry (CV) for **CoZn**, **CoCo**, **ZnZn**, **Co**, and **Zn** are shown in Figures S5 and S6, respectively. As shown in Figure S6, the redox potential of Co^{II}Zn^{II}/Co^{I}Zn^{II} in **CoZn** (-0.87 V) is more positive than that of Co$_2^{II,II}$/Co$_2^{I,II}$ in **CoCo** (-0.94 V) under CO_2 atmosphere, indicating Co^{II} in **CoZn** is easier to be reduced than that in **CoCo**.

The photocatalytic experiments of CO_2 reduction by **CoZn** were performed under the same conditions as those previously described

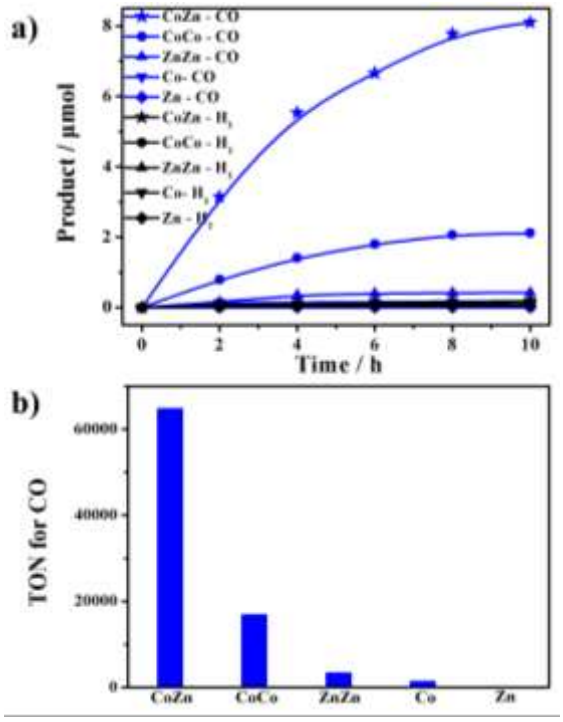

Figure 2. The results of photocatalytic reduction of CO_2 to CO by **CoZn, CoCo, ZnZn, Co**, and **Zn** under the same conditions. a) Time-dependent photocatalytic evolution of CO (blue) and H_2 (black) catalyzed by **CoZn** (★, 0.025 μM), **CoCo** (●, 0.025 μM), **ZnZn** (▲, 0.025 μM), **Co** (▼, 0.025 μM) and **Zn** (◆, 0.025 μM), respectively, under the irradiation of a LED light (450 nm, 100 mW·cm^{-2}, irradiation area, 0.8 cm^2) in the presence of [Ru(phen)$_3$](PF$_6$)$_2$ (0.4 mM) and TEOA (0.3 M) in 5 mL CO_2-saturated H_2O/CH_3CN (v/v = 1:4) solution at 25 ºC. To confirm the reliability of the data, each photocatalytic reaction was repeated at least three times. b) A comparison of photocatalytic activity of **CoZn** with **CoCo**, **ZnZn**, **Co**, and **Zn**.

Table 1. The results of photocatalytic reduction of CO_2 to CO by different catalysts under the same conditions.[a]

Entry	Cat.	Conc (μM)	CO (μmol)	H_2 (μmol)	CO%	TON for CO	TOF for CO (s^{-1})
1	**CoZn**	0.025	8.10	0.16	98%	65000	1.8
2	**CoCo**	0.025	2.11	0.046	98%	17000	0.47
3	**ZnZn**	0.025	0.42	0.17	71%	3400	0.093
4	**Co**	0.025	0.18	0.063	74%	1500	0.040
5	**Zn**	0.025	0	0.050	0	0	0

[a] Reaction conditions: [Ru(phen)$_3$](PF$_6$)$_2$ (0.4 mM), TEOA (0.3 M), H_2O/CH_3CN (v/v = 1:4), LED light (450 nm, 100 mW·cm^{-2}, irradiation area 0.8 cm^2), 10 h, 25 °C. TON and TOF values for CO were calculated based on per molecular formula and averaged over three reactions, with deviations below 5% for Entry 1, and 2, and about 10 % for Entry 3, 4 and 5.

for **CoCo** and **Co**.[18] Typically, a 5 mL CO_2-saturated H_2O/CH_3CN solution (v/v = 1:4) containing certain amount of **CoZn-a** catalyst, [Ru(phen)$_3$](PF$_6$)$_2$ photosensitizer (PS) and triethanolamine (TEOA) sacrificial reductant was irradiated by a LED light (450 nm, 100 mW·cm^{-2}) at 25 ºC. The generated gases were analyzed by gas chromatography (GC). The results show that one single photoredox cycle produces 8.10 μmol of CO and 0.16 μmol of H_2 within 10 h (Table 1, Entry 1; Figure 2a), along with trace amount of formate detected in the liquid phase by ion chromatograph (IC). The

Angewandte Communications

amounts of gases generated correspond to the selectivity to CO of 98%, and the TON and TOF values for CO of 65000 and 1.80 s^{-1}, respectively (Table 1, Entry 1). This TON value is 4-, 19- and 45-fold higher than those of **CoCo** (17000), **ZnZn** (3400), and **Co** (1500) under the same conditions (Table 1, Entry 2-4; Figure 2b). The quantum yield of **CoZn** to CO was determined to be 0.15 % (see SI), 4-fold higher than that of **CoCo** (0.04%).[18] Moreover, when the solutions containing 0.05 and 0.1 mM of **CoZn** were irradiated with LED light for 5 min, much high quantum yields of 4.0% and 4.6% were obtained (see SI). The above results illustrate that after the replacement of one Co^{II} in **CoCo** with a Zn^{II}, the resulted **CoZn** exhibits significantly enhanced photocatalytic activity for CO_2-to-CO conversion. As the mononuclear zinc complex of $[ZnL^2(CH_3CN)](ClO_4)_2$ (**Zn**) shows no catalytic activity under the same conditions (Table 1, Entry 5), the extremely higher photocatalytic activity of **CoZn** over **CoCo** can evidence directly that there is a strong synergistic catalysis effect between Co^{II} and Zn^{II} within **CoZn**. This result, together with the much higher TON values of **CoCo** over **Co**, and **ZnZn** over **Zn** (Table 1, Entry 2-5), solidly illustrate that there is a DMSC effect between two metals within dinuclear metal cryptates, that is, Co^{II} acts as a catalytic centre, and Zn^{II} serves as an assistant catalytic site to facilitate the cleavage of C-O bond of the O=C-OH intermediate.

To see if the photocatalytic activity for CO_2 reduction can be boosted simply by adding Zn^{2+} as a Lewis acid to the reaction system containing dinuclear **CoCo** or mononuclear **Co** catalyst, as observed in the electrocatalytic CO_2 reduction by mononuclear metal catalysts,[15-17] the experiments of photocatalytic CO_2 reduction by **CoCo** and **Co** in the presence of Zn^{II} were performed. As shown in Table S3, the addition of Zn^{2+}/Mg^{2+}/Li^+ as a Lewis acid to the reaction systems containing **CoCo** or **Co** catalyst cannot boost and even slightly decrease the CO_2 reduction catalytic activity of **CoCo** and **Co**. The above results clearly demonstrate that the externally added Lewis acid to the **CoCo**/**Co** photocatalytic system cannot generate the DMSC effect as **CoZn** behaves, indicating the cryptand ligand (L^1) plays a crucial role for the construction of the highly active **CoZn** catalyst with DMSC effect, in which L^1 can hold Co^{II} and Zn^{II} in a close proximity (5.56 Å) for strong affinity towards CO_2 substrate, while the externally added metal ions has little opportunity to form μ-CO_3 bridged dinuclear complexes with mononuclear **Co** and **Zn** catalysts. Therefore, DMSC effect for photocatalytic CO_2-to-CO conversion can only be produced within a dinuclear metal complexes with suitable M···M distance fixed by an organic ligand for strong affinity towards CO_2 substrate.

A series of control experiments were carried out to thoroughly investigate this photocatalytic reaction of CO_2-to-CO conversion (Table 2). Firstly, the photocatalytic reactions was performed without **CoZn**, $[Ru(phen)_3](PF_6)_2$, TEOA, or visible-light. The results show that without any of these reaction factors, no CO was detected (Table 2, Entry 2-5), suggesting that catalyst, photosensitizer, sacrificial reductant, and light are all indispensible to CO_2-to-CO conversion. It is worthy to note that water is also critical for CO_2-to-CO conversion. No CO was detected in the absence of water (Table 2, Entry 6). Slightly increasing the ratio of H_2O/CH_3CN to 1:9, significant amount of CO (5.5 μmol) was generated, demonstrating that water acts as an effective proton source in the reaction process. When the ratio of H_2O/CH_3CN reached to 1:4, a maximum amount of CO (8.1 μmol) was obtained. Further increase the ratio of H_2O/CH_3CN to 1:1, the generated CO was dramatically decreased, and no CO could be detected in pure water (Table S5, Figure S8), as catalyst and PS can only slightly soluble in water. Secondly, the $^{13}CO_2$ isotope trace experiment was performed to confirm the generated CO coming from the reduction of CO_2. The result clearly illustrates that under a $^{13}CO_2$ atmosphere, the generated gas in the photocatalytic system was ^{13}CO (Figure S9), demonstrating the generated CO originates from the reduction of CO_2 by **CoZn**, rather than the decomposition of the catalyst/photosensitizer/sacrificial reductant. Thirdly, a mercury poison test was carried out to make certain that the catalytic reaction is homogeneous. The results show that the amount of CO generated from the system in the presence of mercury is almost equal to that without mercury (Table 2, Entry 7), illustrating that the production of CO is catalyzed by **CoZn** rather than metal Co, and the above photocatalytic reaction is homogeneous. Fourthly, the kinetics of this homogeneous photocatalytic reaction was studied. The results illustrate that the amounts of CO evolution are roughly linearly dependent on the concentrations of **CoZn** within 0.00625~0.025 μM range (Figure S10), suggesting that the photochemical reduction of CO_2 to CO is a first-order reaction and only Co(II) in **CoZn** acts as the catalytic center.

Table 2. The Results of Control Experiments for the Photocatalytic Reduction of CO_2 to CO.[a]

Entry	Cat.	Conc (μM)	CO (μmol)	H_2 (μmol)	CO%	TON for CO	TOF for CO (s^{-1})
1	**CoZn**	0.025	8.10	0.16	98%	65000	1.8
2	0	0	0	0.049	0	0	0
3	**CoZn**	0.025	0	0	0	0	0
4	**CoZn**	0.025	0	0.11	0	0	0
5	**CoZn**	0.025	0	0	0	0	0
6	**CoZn**	0.025	0	0.10	0	0	0
7	**CoZn**	0.025	7.98	0.16	98%	64000	1.7

[a] Reaction conditions: $[Ru(phen)_3](PF_6)_2$ (0.4 mM), TEOA (0.3 M), H_2O/CH_3CN (v/v = 1:4), LED light (450 nm, 100 mW·cm^{-2}, irradiation area 0.8 cm^2), 10 h, 25 °C. TON and TOF values are averaged over three reactions, with deviations below 5%. 2: without **CoZn**; 3: without $[Ru(phen)_3](PF_6)_2$; 4: without TEOA; 5: without visible light; 6: without H_2O; 7: adding 0.5 mL of Hg.

The stability of **CoZn** catalyst during the photocatalytic CO_2 reduction reaction was investigated by the durability test and dynamic light scattering (DLS) measurement. The durability test for **CoZn** shows that the addition of $[Ru(phen)_3](PF_6)_2$ can reactivate the reaction of photochemical CO_2-to-CO conversion reaction that is nearly ceased (Figure S11), indicating that the cease of CO_2 reduction reaction is attributed to the photo-degradation of $[Ru(phen)_3](PF_6)_2$ rather than the inactivation of **CoZn** catalyst. The dynamic light scattering (DLS) measurement indicates that no nanoparticle generated in the solution after the CO_2 reduction reaction, revealing that **CoZn** does not decompose during the process of photocatalytic CO_2 reduction. Therefore, both the durability test and DLS measurement have demonstrated that **CoZn** possesses a good stability and can serve as a stable homogeneous catalyst for photochemical CO_2 reduction to CO.

The fluorescence quenching studies were carried out on the reaction system containing $[Ru(phen)_3]^{2+}$ photosensitizer (PS) with various concentrations of **CoZn** catalyst or TEOA sacrificial reductant in a degassed solution of H_2O/CH_3CN (*v*/*v* = 1:4). As shown in Figure S12, the fluorescent intensity of $[Ru(phen)_3]^{2+}$ was decreased even with the addition of small amount of **CoZn** catalyst (Figures S12a and b), while no obvious change was observed with the addition of even much excessive TEOA (0.3 M) (Figures S12e and 12f). Moreover, transient absorption spectra of $[Ru(phen)_3](PF_6)_2$ in the presence of TEOA and **CoZn-a** were

Angewandte Communications

measured (Figure S13), which indicate new species, most probably $[Ru(phen)_3]^{3+}$ was formed in the presence of **CoZn-a**, while no obvious change with the addition of TEOA. The above results demonstrate the $[Ru(phen)_3]^{2+}$* is quenched through the following oxidative pathway:[33]

$Co^{II}Zn^{II}$-a + $Ru(phen)_3]^{2+}$* → **$Co^{I}Zn^{II}$-b** + $[Ru(phen)_3]^{3+}$

$[Ru(phen)_3]^{3+}$ + TEOA → $[Ru(phen)_3]^{2+}$ + $TEOA^+$

Stern-Volmer analysis from the data in Figure S12c revealed that the rate constant for electron transfer from $[Ru(phen)_3]^{2+}$* to **CoZn-a** is $k_q = 3.0 \times 10^{10}$ M^{-1} s^{-1}, indicating a diffusion-controlled electron transfer process. Indeed, the redox potential of $[Ru(phen)_3]^{3+/2+}$* (-0.84 V, see SI) is negative than the $Co^{2+/+}Zn$ onset reduction potential of **CoZn** (-0.58 V), and close to its redox potential of -0.87 V (Figure S6a), indicating the electron transfer from $[Ru(phen)_3]^{2+}$* to $Co^{II}Zn^{II}$ is thermodynamically accessible.

To well understand the dramatically enhanced photocatalytic activity of **CoZn** towards CO_2-to-CO conversion compared to **CoCo**, the catalytic mechanism was investigated at a molecular level by the DFT calculations (see SI), and compared with the energy diagram for the reaction pathway of **CoCo** (Figure S15). As shown in Figure 3, firstly, **CoZn** rapidly captures the CO_2 substrate to form a carbonate-bridged complex of **CoZn-a**, as observed from the experimental results. Secondly, **CoZn-a** obtains one electron from $[Ru(phen)_3]^{2+}$* to generate **CoZn-b**, during which the $Co^{II}Zn^{II}$ in **CoZn-a** was reduced to $Co^{I}Zn^{II}$. Thirdly, **CoZn-b** is protonated to yield **CoZn-c** after elimination of a water molecule, and then the CO_2 in **CoZn-c** accepts $2e^-$ from Co^I to be reduced to CO_2^{2-} through the transition state of **TS1-CoZn** to generate **CoZn-d**. The total energy barrier for this transition state is only 6.55 kcal/mol, much lower than the corresponding values of **CoCo** (10.41 kcal/mol) and **Co** (24.96 kcal/mol) (Figures 4 and S15). Fourthly, Co^{III} in **CoZn-d** is reduced to Co^{II} by $[Ru(phen)_3]^{2+}$* through a PCET oxidative process to form **CoZn-e**. Finally, the C-OH bond of $COOH^-$ within **CoZn-e** is cleaved by the DMSC interaction *via* the second transition state **TS2-CoZn** to generate **CoZn-f**, where Zn^{II} binds to OH^- and Co^{II} binds to CO. The total energy barrier calculated for **TS2-CoZn** is as low as 13.99 kcal/mol, also much lower than the corresponding values of **CoCo** (16.35 kcal/mol) and **Co** (20.73 kcal/mol) (Figures 4 and S15). After the release of CO in **CoZn-f**, **CoZn** is regenerated and the photocatalytic cycle restarts. From Figure 3 it can be found that the reactions of CO_2 reduction contain several proton-participated reaction process, and the energy barriers become much higher without the participation of protons, this result is consistent with the experimental observation that water is critical for CO_2-to-CO conversion (Table 2, Entry 6).

The above results of DFT calculations strongly support the experimental observations that the TON value of **CoZn** is much higher than those of **CoCo** and **Co** under the same conditions (Table 1). As the selected natural bond orbital (NBO) charge of Zn in **CoZn** (1.280e) is more positive than that of Co in **CoCo** (1.115e, Table S6), the significantly improved photocatalytic performance of **CoZn** over **CoCo** can be ascribed to the stronger binding affinity of Zn^{II} to OH^- over Co^{II}, which enormously strengthens the DMSC effect between Co^{II} and Zn^{II} in **CoZn**, thus greatly promotes the cleavage of the C-OH bond in O=C-OH intermediate, and significantly accelerates the photochemical reduction reaction of CO_2 to CO.

In summary, by replacing one Co^{II} in **CoCo** with a Zn^{II}, we have successfully obtained a dinuclear heterometallic **CoZn** catalyst, which shows greatly enhanced activity for photochemical reduction of CO_2 to CO in a water-containing reaction system under a visible

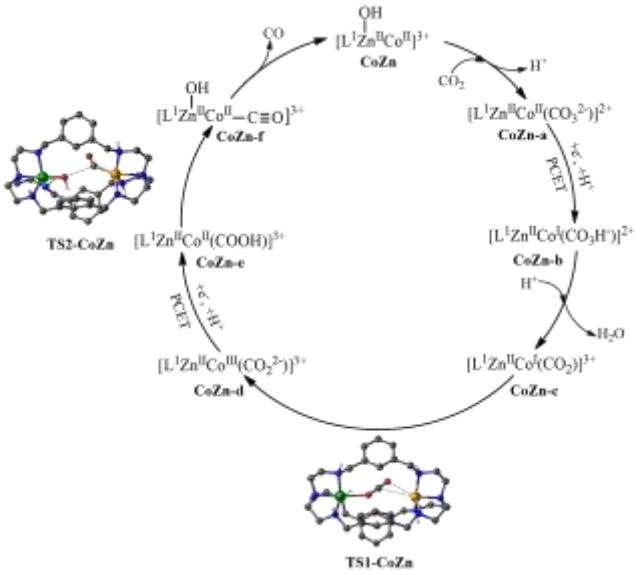

Figure 3. Proposed catalytic mechanism of **CoZn** for the reduction of CO_2 to CO driven by visible-light.

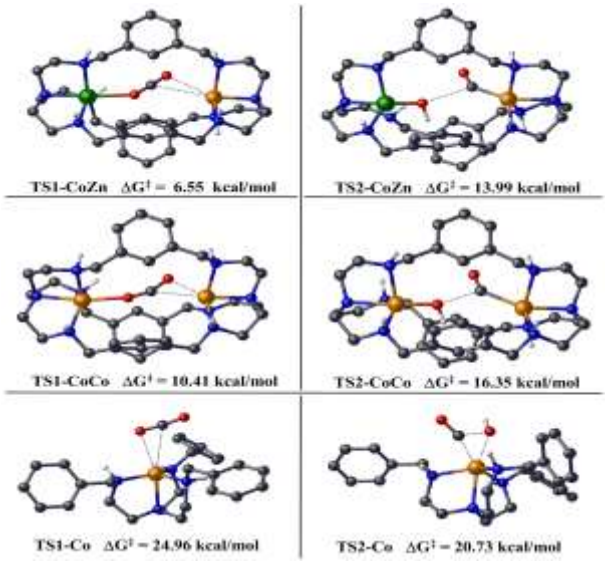

Figure 4. The energy barriers of two transition states for **CoZn**, **CoCo**, and **Co**.

light irradiation with a low light intensity of 100 $mW \cdot cm^{-2}$. The TON and TOF values reach fantastic 65000 and 1.8 s^{-1}, respectively, and the selectivity to CO reaches as high as 98%. The greatly enhanced catalytic activity of **CoZn** can be ascribed to significantly strengthened DMSC effect between Co^{II} and Zn^{II}, where the assistant catalytic site of Zn^{II} shows much strong binding affinity to OH^-, greatly promoting the C-OH cleavage of O=C-OH intermediate, thus significantly enhancing the photocatalytic activity of **CoZn** for CO_2 reduction to CO. This research has not only directly evidenced the DMSC effect within dinuclear metal cryptates, but also developed a homogeneous catalyst with unprecedented high activity and selectivity for photocatalytic reduction of CO_2 to CO in a water-containing reaction system. The results presented here provide a new strategy for the design and synthesis of high efficient, high selective, stable and cheap photocatalysts for CO_2-to-CO conversion, and the concept of evidenced DMSC will greatly boost

the developments of 'artificial photosynthesis' and other dinuclear metal catalysts.

Acknowledgements

This work was supported by National Key R&D Program of China (2017YFA0700104), the NSFC (21790052 and 21331007), and the 111 Project (D17003).

Received: ((will be filled in by the editorial staff))
Published online on ((will be filled in by the editorial staff))

Keywords: CO_2 reduction • dinuclear metal complex • synergistic catalysis • homogeneous catalyst • DFT calculations

[1] Y. Hayashi, S. Santoro, Y. Azuma, F. Himo, T. Ohshima, K. Mashima, *J. Am. Chem. Soc.* **2013**, *135*, 6192-6199.
[2] A. Magnuson, M. Anderlund, O. Johansson, P. Lindblad, R. Lomoth, T. Polivka, S. Ott, K. Stensjo, S. Styring, V. Sundstrom, L. Hammarstrom, *Acc. Chem. Res.* **2009**, *42*, 1899-1909.
[3] O. Iranzo, A. Y. Kovalevsky, J. R. Morrow, J. P. Richard, *J. Am. Chem. Soc.* **2003**, *125*, 1988-1993.
[4] L. Zong, C. Wang, A. M. Moeljadi, X. Ye, R. Ganguly, Y. Li, H. Hirao, C. H. Tan, *Nat. Commun.* **2016**, *7*, 13455.
[5] N. P. Mankad, *Chem. Eur. J.* **2016**, *22*, 5822-5829.
[6] J. B. Vincent, G. L. Olivier-Lilley, B. A. Averill, *Chem. Rev.* **1990**, *90*, 1447-1467.
[7] L. Que, Jr., W. B. Tolman, *Nature* **2008**, *455*, 333-340.
[8] D. C. Zhong, T. B. Lu, *Chem. Commun.* **2016**, *52*, 10322-10337;
[9] J. M. Stauber, E. D. Bloch, K. D. Vogiatzis, S. L. Zheng, R. G. Hadt, D. Hayes, L. X. Chen, L. Gagliardi, D. G. Nocera, C. C. Cummins, *J. Am. Chem. Soc.* **2015**, *137*, 15354-15357.
[10] D. Huang, R. H. Holm, *J. Am. Chem. Soc.* **2010**, *132*, 4693-4701.
[11] T. B. Lu, X. M. Zhuang, Y. W. Li, S. Chen, *J. Am. Chem. Soc.*, **2004**, *126*, 4760-4761.
[12] J. M. Chen, W. Wei, X. L. Feng, T. B. Lu, *Chem. Asian J.*, **2007**, *2*, 710-719.
[13] R. Angamuthu, P. Byers, M. Lutz, A. L. Spek, E. Bouwman, *Science* **2010**, *327*, 313-315.
[14] L. M. Cao, H. H. Huang, J. W. Wang, D. C. Zhong, T. B. Lu, *Green Chem.* **2018**, *20*, 798-803.
[15] I. Azcarate, C. Costentin, M. Robert, J. M. Savéant, *J. Am. Chem. Soc.* **2016**, *138*, 16639−16644.
[16] M. D. Sampson, C. P. Kubiak, *J. Am. Chem. Soc.* **2016**, *138*, 1386−1393.
[17] A. Zhanaidarova, H. Steger, M. H. Reineke, C. P. Kubiak, *Dalton Trans.* **2017**, *46*, 12413-12416.
[18] (a) T. Ouyang, H. H. Huang, J. W. Wang, D. C. Zhong, T. B. Lu, *Angew. Chem. Int. Ed.* **2017**, *56*, 738-743; (b) Z. A. Lan, X. C. Wang, *Acta Phys. -Chim. Sin.*. **2017**, *33*, 457-457.
[19] H. Rao, J. Bonin, M. Robert, *Chem. Commun.* **2017**, *53*, 2830-2833.
[20] A. Rosas-Hernandez, C. Steinlechner, H. Junge, M. Beller, *Green Chem.* **2017**, *19*, 2356-2360.
[21] R. Schlogl, *Angew. Chem. Int. Ed.* **2011**, *50*, 6424-6426.
[22] E. E. Benson, C. P. Kubiak, A. J. Sathrum, J. M. Smieja, *Chem. Soc. Rev.* **2009**, *38*, 89-99.
[23] C. D. Windle, R. N. Perutz, *Coord. Chem. Rev.* **2012**, *256*, 2562-2570.
[24] S. Wang, X. Wang, *Angew. Chem. Int. Ed*. **2016**, *55*, 2308-2320.
[25] F. Studt, I. Sharafutdinov, F. Abild-Pedersen, C. F. Elkjaer, J. S. Hummelshoj, S. Dahl, I. Chorkendorff, J. K. Norskov, *Nat. Chem.* **2014**, *6*, 320-324.
[26] V. S. Thoi, N. Kornienko, C. G. Margarit, P. Yang, C. J. Chang, *J. Am. Chem. Soc*. **2013**, *135*, 14413-14424.
[27] L. Chen, Z. Guo, X.-G. Wei, C. Gallenkamp, J. Bonin, E. Anxolabéhère-Mallart, K.-C. Lau, T.-C. Lau, M. Robert, *J. Am. Chem. Soc.* **2015**, *137*, 10918-10921.
[28] E. Fujita, *Coord. Chem. Rev*. **1999**, *185-186*, 373-384.
[29] H. Takeda, K. Ohashi, A. Sekine, O. Ishitani, *J. Am. Chem. Soc.* **2016**, *138*, 4354-4357.
[30] J. Bonin, M. Robert, M. Routier, *J. Am. Chem. Soc.* **2014**, *136*, 16768-16771.
[31] S. Sato, T. Morikawa, T. Kajino, O. Ishitani, *Angew. Chem. Int. Ed.* **2013**, *52*, 988-992.
[32] Z. Guo, F. Yu, Y. Yang, C. F. Leung, S. M. Ng, C. C. Ko, C. Cometto, T. C. Lau, M. Robert, *ChemSusChem* **2017**, *10*, 4009-4013.
[33] G. J. Kavarnos, N. J. Turro, *Chem. Rev.* 1986, *86*, 401-449.

10.1002/anie.201811010

Angewandte Communications

CO_2 Reduction

Ting Ouyang, Hong-Juan Wang, Hai-Hua Huang, Jia-Wei Wang, Song Guo, Wen-Ju Liu, Di-Chang Zhong*, and Tong-Bu Lu*

_____ **Page – Page**

Dinuclear Metal Synergistic Catalysis Boosts Photochemical CO_2-to-CO Conversion

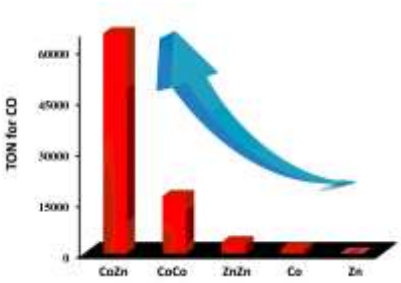

*A dinuclear heterometallic **CoZn** catalyst shows much higher photocatalytic activity than the corresponding dinuclear homometallic **CoCo** and **ZnZn** catalysts, as well as mononuclear **Co** and **Zn** catalysts for CO_2 reduction under the same conditions. The increased photocatalytic performance of **CoZn** catalyst is due to the enhanced dinuclear metal synergistic catalysis (DMSC) effect between Zn^{II} and Co^{II}, which dramatically lowers the activation barriers of both transition states of CO_2 reduction.*